Tuberculosis 115 (2019) 113–120

Contents lists available at ScienceDirect

Tuberculosis

journal homepage: www.elsevier.com/locate/tube

Dysregulation of key cytokines may contribute to increased susceptibility of diabetic mice to *Mycobacterium bovis* BCG infection

Md Abdul Alim[a,*], Suchandan Sikder[a], Harindra Sathkumara[a], Andreas Kupz[b], Catherine M. Rush[a], Brenda L. Govan[a], Natkunam Ketheesan[c]

[a] College of Public Health, Medical and Veterinary Sciences, Australian Institute of Tropical Health and Medicine, James Cook University, Townsville, Queensland, Australia
[b] Australian Institute of Tropical Health and Medicine, James Cook University, Cairns, Queensland, Australia
[c] School of Science & Technology, University of New England, New South Wales, Australia

ARTICLE INFO

Keywords:
Bacille Calmette-Guérin
Murine model
Macrophage
Phagocytosis
Type 2 diabetes
Tuberculosis

ABSTRACT

Diabetes is one of the major co-morbidities contributing to the high global burden of tuberculosis (TB). The increased susceptibility of individuals with type 2 diabetes (T2D) to TB is multifactorial and may influence the efficacy of vaccines. This study was undertaken to determine the early immune responses that occur following infection with *Mycobacterium bovis* Bacille Calmette-Guérin (BCG) in a diet-induced murine model of T2D. The phagocytic capabilities of alveolar (AM) and resident peritoneal macrophages (RPM) were assessed using *ex vivo* assays. Compared to macrophages from non-diabetic mice, macrophages from diabetic animals showed decreased BCG uptake and killing and inflammatory cytokine production (TNF-α, MCP-1, IL-6, IL-1β). *In vivo* susceptibility to BCG was determined following intravenous infection and diabetic mice showed a trend towards increased mortality, higher bacterial burden in the lung, liver and spleen and increased inflammatory lesions compared to controls. Differences between tissue cytokines were observed as early as one day post-infection and by days 14 and 35, lung and liver TNF-α and IFN-γ levels were decreased in diabetic mice compared to controls. These results suggest that early dysregulated immune responses may influence the susceptibility of T2D mice to BCG infection.

1. Introduction

The global burden of Type 2 diabetes (T2D) has increased significantly over the past 50 years [1]. T2D results in a three to four-fold increased risk of developing tuberculosis (TB) [2], other mycobacterial infections [3,4] and reactivation of latent TB (LTBI) [5]. *Mycobacterium bovis* Bacillus Calmette–Guérin (BCG) is the only TB vaccine. BCG prevents childhood TB, but the level of protection in adults varies from 0 to 80% [6,7]. Intravenous BCG vaccination has shown improved protection against TB in non-human primates [8–10]. The impact of T2D in BCG vaccination efficacy is unknown.

To explore the potential defects resulting in increased susceptibility of diabetics to mycobacterial infections and to investigate the impact of diabetes on intravenous BCG vaccination, appropriate animal models that reflect the pathophysiological mechanisms observed in T2D are crucial. The animal models that have been previously used to study mycobacterial infection-diabetes co-morbidity were based on genetic modifications or chemical alteration of pancreatic β-cell function, which more closely model type 1 diabetes [11–18]. Furthermore, some of previously used diet-induced animal models have not been very representative of T2D due to the use of less appropriate dietary composition [19] and short dietary intervention period [20]. These are not conducive to the development of overt clinical signs of diabetes and its associated macro- and microvascular complications. To overcome some of these shortcomings we previously characterized a more robust diet-induced murine model of T2D using an energy-dense diet [3,21]. In the current study, we used BCG to investigate the antimycobacterial functions of murine diabetic versus non-diabetic macrophages, and whether diabetes influences survival and tissue bacterial burden, inflammation and cytokine level following intravenous BCG infection. We show that dysregulated tissue cytokines may render the T2D host to a greater susceptibility to mycobacterial infection.

* Corresponding author. Department of Pathology and Parasitology, Faculty of Veterinary Medicine, Chittagong Veterinary and Animal Sciences University, Khulshi, Chittagong, 4225, Bangladesh.
E-mail addresses: mdabdul.alim@my.jcu.edu.au (M.A. Alim), suchandan.sikder@my.jcu.edu.au (S. Sikder), harindra.sathkumaramudiyanselage@my.jcu.edu.au (H. Sathkumara), andreas.kupz@jcu.edu.au (A. Kupz), catherine.rush@jcu.edu.au (C.M. Rush), brenda.govan@jcu.edu.au (B.L. Govan), nkethees@une.edu.au (N. Ketheesan).

https://doi.org/10.1016/j.tube.2019.02.005
Received 22 October 2018; Received in revised form 11 February 2019; Accepted 17 February 2019

2. Materials and methods

2.1. Induction of diet-induced murine model of type 2 diabetes

Six-week-old male C57BL/6 mice were used for the induction of type 2 diabetes as previously described [3,21]. One group of mice received *ad libitum* access to an energy dense-diet (EDD), while the control group received a standard rodent diet (SRD) [21]. After 30 weeks of respective diets, glucose tolerance tests (GTT) were used to assess insulin resistance (Supplementary Fig. 1) [21,22].

2.2. Bacterial isolate and culture

Mycobacterium bovis BCG was kindly provided by Dr Nick West, School of Chemistry and Molecular Biosciences, The University of Queensland, Australia. The bacterial stock was grown on 7H9 medium containing 0.05% Tween 80 and supplemented with 10% OADC (Oleic Albumin Dextrose Catalase) to mid-log phase and stored at −80 °C until use.

2.3. Internalization and killing assay

The capacities of murine diabetic and control alveolar macrophages (AM) and resident (non-elicited) peritoneal macrophages (RPM) to engulf and kill *M. bovis* BCG were evaluated using standard methods [3]. Broncho-alveolar lavage fluid (BALF) and peritoneal exudates were pooled from each group of animals (n = 30/group) prior to isolation of macrophages. $CD11c^+$ cells (AM) were isolated from BALF by positive selection using the EasySep™ Mouse CD11c positive selection kit (STEMCELL™ technologies) according to the manufacturer's instructions. $CD11b^+$ cells (RPM) were prepared from peritoneal exudate fluid using anti-CD11b Magnetic Particles-DM (BD Biosciences, Australia) according to the manufacturer's instructions. The purity of both $CD11c^+$ and $CD11b^+$ cells was assessed using the BD FACSCalibur™ flow cytometer and found to be > 90% (data not shown). The magnetically sorted cell suspensions were resuspended in RPMI 1640 (Invitrogen, Australia) culture media at a concentration of 1×10^5 cells/well in 1 mL in 48 well cell culture plates. Internalization, killing and cytokine production were measured at 4 h and 24 and/or 48 h, according to previously described methods [3]. Briefly, three to five replicate wells were used for each group at each timepoint. *M. bovis* BCG was added to wells at an MOI 1:10 and incubated at 37 °C with 5% CO_2. After 4 h of co-culture, supernatants were collected for cytokine determination. The wells were treated with Amikacin (200 μg/mL) for 2 h to kill extracellular bacteria followed by washing with phosphate buffered saline (PBS, pH 7.2). To determine the killing after 24 and/or 48 h, other plates were treated and incubated as described above. All the wells were treated with Trition X-100® (0.1%, Sigma, Australia) for 10 min and washed by centrifugation. For enumeration of colony forming unit (CFU), serial 10-fold dilutions were prepared with the cell lysates and plated on 7H11 agar plates. Mycobacterial uptake by macrophages was calculated based on the number of bacteria internalized after 4 h in comparison to bacteria added per well. Macrophage killing capability was determined by normalizing CFU at 24 and 48 h based on uptake at 4 h.

$$4\,h\ uptake = \frac{(No.\ of\ internalized\ bacteria\ after\ 4\,h)}{(No.\ of\ bacteria\ added)} X100$$

$$24\ or\ 48\,h\ survival = \frac{(\,No.\ of\ survived\ \ bacteria\ \ after\ 24/48\,h)}{(No.\ of\ bacteria\ internalized\ after\ 4\,h)} X100$$

2.4. Bacterial infections

For *in vivo* infections, frozen aliquots of *M. bovis* BCG were prepared for injection as previously described [3,23]. Briefly, frozen bacterial stocks of known concentration (CFU/mL) were thawed and washed twice with PBS by centrifugation at 4000 × *g* for 10 min. Pellets were resuspended in PBS, vortexed and clumps were disaggregated by passing the bacterial suspension through 29-gauge needles 10–15 times followed by water-bath sonication for 10 s. Serial dilutions of the resulting suspension were plated on 7H11 agar plates to retrospectively enumerate the precise CFU/mL of the inoculum. Diabetic and control mice were infected intravenously via the tail vain [3,24]. For 60 day survival experiments mice (n = 9–12/group) were infected with 2×10^6 CFU and mice were observed daily. Moribund mice were euthanized by CO_2 asphyxiation and survival was recorded. The kinetics of infection were assessed at days 1, 14 and 35 following infection with 1×10^6 CFU (n = 4–5/group/timepoint).

2.5. Preparation of organ homogenates

At days 1, 14, and 35, 4–5 mice from each experimental group were euthanized by CO_2 asphyxiation for the collection of lung, liver and spleen. All samples were processed according to published protocols [3,12,25]. Briefly, lung (left lobe), liver (1 g) and spleen (half of total organ weight) were homogenized separately in stomacher bags containing 1 mL of PBS with 0.05% Tween 80. The homogenates were centrifuged, and the supernatants were collected and stored at −80 °C for cytokine assays. The cell pellets were then lysed using 0.1% Triton X-100® for 10 min. Serial 10-fold dilutions were prepared from lysates and plated on 7H11 agar plates. Colonies were counted after 2–3 weeks of incubation at 37 °C with 5% CO_2.

2.6. Histopathological examinations

Lung, liver and spleen of *M. bovis* BCG-infected mice were weighed at 1, 14, 35 days post-infection (dpi). For histopathological examination, the right lung lobes and liver (after removing 1 g for bacterial counts) were collected in 10% neutral buffered formalin. Tissue sections of lung and liver were prepared from formalin fixed tissue and stained with Haematoxylin and Eosin (H&E). The relative percentage of inflamed area within the lung was evaluated on representative lung sections according to previously published methods [26]. The inflamed area was calculated on the same lung sections by capturing images using 100x magnification. The inflamed areas within the liver were quantified according to previously described methods [3,27,28]. The CellSens® Image Analysis software (Olympus) was used for digital photography and quantitative analysis of the tissue sections.

2.7. Tissue Ziehl-Neelsen staining for localization of bacteria

Ziehl-Neelsen (ZN) staining of liver sections was performed at 14 and 35 dpi. Counting of acid-fast bacilli was done using previously published protocols [28]. In short, a representative liver section from each mouse was stained and visualized at 1000x magnification and the number of ZN positive magenta bacilli within each of the inflammatory focus/granuloma was counted. Inflammatory lesions showing at least one ZN positive bacillus were identified and the total number of individual bacilli within 10 such lesions were enumerated.

2.8. Measurement of cytokines

Inflammatory cytokine concentrations in organ homogenates and cell culture supernatants were determined using the BD Cytometric Bead Array Mouse Inflammation Kit® (TNF-α, IL-6, MCP-1, IL-10, IL-12p70, IFN-γ), Mouse Th1/Th2/Th17 Cytokine Kit® (IL-2, IL-4, IL-17A) and Mouse IL-1β Flex Set® (BD Bioscience, Australia). Manufacturer's instructions were followed to assess the cytokine levels. Data were acquired on a BD FACSCalibur™ flow cytometer using BD CellQuest® software and analysed by BD FCAP Array ™ software (version 3.0).

2.9. Statistical analysis

Statistical analysis was performed using SPSS version 24.0 and GraphPad Prism 7.03 software. Normally distributed data were compared between groups using the unpaired *t*-test with Welch's correction. Normally distributed data of multiple groups were compared using the ordinary one-way ANOVA with Holm-Sidak's multiple comparisons test. Non-normally distributed data were compared between the groups using the non-parametric Mann-Whitney *U* test. The Kruskal-Wallis test with Dunn's multiple comparisons was performed for non-normally distributed data of multiple groups. A two-way ANOVA with Sidak's multiple comparisons test was performed for data from repetitive measures (e.g. glucose tolerance test). Kaplan Meier survival curves with log-rank (Mantel-Cox) tests were used to compare diabetic and control mouse survival. All data were presented as mean ± SEM (Standard Error of the Mean). The level of significance was indicated as $^{*}P \leq 0.05$, $^{**}P \leq 0.01$, $^{***}P \leq 0.001$ and $^{****}P \leq 0.0001$.

3. Results

3.1. Phagocytosis and ex vivo cytokine production by macrophages are impaired in Mycobacterium bovis BCG-infected T2D mice

We first investigated whether the phagocytic and killing capacities of murine diabetic and non-diabetic control macrophages differed. After 4 h of co-culture, the internalization of *M. bovis* BCG by alveolar macrophages (AM) from diabetic mice was 26% lower compared to controls (Fig. 1A). Killing of *M. bovis* BCG by AM from diabetic mice after 24 h of co-culture was 4% lower compared to controls (Fig. 1B). Similarly, the bacterial uptake by resident peritoneal macrophages (RPM) from diabetic mice was 34% lower compared to control macrophages (Fig. 1D). Although the killing capacity of RPM increased over time, the killing efficiency after 24 h (Fig. 1E) and 48 h (Fig. 1G) of co-culture remained 3.9 and 2.5% lower, respectively in RPM from diabetic mice compared to controls.

We also assessed cytokine levels after co-culture of isolated AM and RPM with *M. bovis* BCG. TNF-α production by AM increased between 4 and 24 h of co-culture (Fig. 1C). Compared to control mice, AM from diabetic mice produced less TNF-α at both the 4 h (control, 69.76 ± 0.57 *vs* diabetic, 44.41 ± 6.14, pg/mL, $P = 0.1062$) and 24 h timepoints (Fig. 1C). The opposite trend was observed for IL-6 production. AM from diabetic mice released more IL-6 in response to BCG at 4 h (control, 4.00 ± 3.15 *vs* diabetic, 17.64 ± 2.29, pg/mL, $P = 0.0096$) and 24 h (Fig. 1C). The production of IL-10 by AM from diabetic and control mice was similar at both 4 h and 24 h of co-culture (data not shown). MCP-1 (Fig. 1C), IL-1β (Fig. 1C), IL-12p70 and IFN-γ production was undetectable in AM from both diabetic and control mice at both timepoints. When RPM were co-cultured with *M. bovis* BCG for 4, 24 and 48 h, increasing TNF-α production was observed. TNF-α levels were significantly lower in RPM from diabetic mice at 4 h (control, 129.36 ± 16.54 *vs* diabetic, 47.50 ± 5.54, pg/mL, $P = 0.0005$) and 48 h (Fig. 1H), although concentrations were similar for both groups of mice at 24 h (Fig. 1F). MCP-1 production by RPM from diabetic mice was significantly lower than controls at 24 and 48 h (Fig. 1F and H) and was not detectable at 4 h. In contrast to our results for AM, RPM from diabetic mice produced less IL-6 than control mice at 4 h (control, 601.26 ± 58.55 *vs* diabetic, 168.77 ± 31.78, pg/mL, $P = 0.0001$), 24 h (Fig. 1F) and 48 h (Fig. 1H) of co-culture. There was a reduced amount of IL-1β produced at 24 h and 48 h (Fig. 1F and H) although it was undetectable at 4 h. A higher level of IL-10 was observed in the RPM from control mice than diabetic at 48 h (control, 56.82 ± 4.51 *vs* diabetic, 18.89 ± 1.32, pg/mL, $P \leq 0.0001$) of co-culture although the level was similar at both 4 and 24 h (data not shown). The production of IL-12p70 and IFN-γ by the RPM from both diabetic and control mice was undetectable at all three timepoints.

3.2. Increased trend in mortality of Mycobacterium bovis BCG-infected T2D mice

Next, we investigated if diabetic mice were more susceptible to death following high-dose (2×10^6 CFU/mouse) infection with *M. bovis* BCG. Sixty days after infection 30% of the diabetic mice had succumbed to infection compared to 7.69% of non-diabetic controls (Supplementary Fig. 2). Although this difference did not reach statistical significance ($P = 0.1698$), these data suggest that diabetic mice have a reduced ability to control BCG infection *in vivo*.

3.3. Gross pathology and increased Mycobacterium bovis BCG burden in T2D mice

To assess the immune response and histopathological changes to BCG in more detail, mice were infected with 1×10^6 CFU and were sacrificed at 1, 14 and 35 dpi. Both diabetic and control mice developed spleno- and hepatomegaly (data not shown). Bacterial loads gradually increased in lung and liver of both diabetic and control mice followed by a decline at later timepoints (Fig. 2A and E). Diabetic mice harboured significantly more bacteria at 14 and 35 dpi compared to controls. In the lung, BCG counts peaked at 14 dpi with diabetic mice showing 2.2-fold more bacteria compared to controls and 2.9-fold more bacteria at 35 dpi (Fig. 2A). Increased bacterial burden was also observed in the liver of diabetic mice with 3.4 and 6.1-fold higher BCG counts at 14 and 35 dpi, respectively (Fig. 2E). Similarly, bacillary burden was 2.5 and 1.8-fold higher in the spleen of diabetic mice compared to controls at 14 and 35 dpi, respectively (data not shown).

3.4. Increased inflammatory responses in Mycobacterium bovis BCG-infected T2D mice

Examination of H&E stained lung sections of BCG-infected mice revealed increased numbers of inflammatory lesions in diabetic mice compared to controls (Fig. 2B, C & D). A diffuse accumulation of inflammatory cells was observed in both diabetic and control groups at 1 dpi (data not shown). At 14 dpi, diabetic mice had 1.6-fold increase of inflamed area across the lung sections compared to controls (Fig. 2B). A similar trend was observed at 35 dpi (Fig. 2B, C & D).

Liver inflammation was also higher in BCG-infected diabetic mice compared to controls (Fig. 2F, G & H). At 1 dpi, a diffuse infiltration of inflammatory cells was observed in the livers of both diabetic and control mice (data not shown) followed by the formation of inflammatory foci/granulomas at later timepoints. The number of inflammatory foci/granulomas in the liver was higher in diabetic mice compared to controls at both 14 (control, 4.40 ± 0.43 *vs* diabetic, 6.68 ± 0.44/section/mouse, $P = 0.0059$) and 35 dpi (control, 6.82 ± 0.46 *vs* diabetic, 8.08 ± 0.78/section/mouse, $P = 0.2010$). The mean area of each inflammatory focus/granuloma was 1.2 and 1.4-fold higher in diabetic mice compared to controls at 14 and 35 dpi, respectively, although this was not statistically significant (data not shown). The overall area of liver inflammation was 1.8 and 1.3-fold higher in diabetic mice compared to controls at both 14 and 35 dpi, respectively (Fig. 2F, G & H). Furthermore, ZN staining of these liver sections demonstrated higher numbers of bacilli per inflammatory focus/granuloma in diabetic mice compared to controls at both 14 (control, 13.00 ± 1.08 *vs* diabetic, 17.56 ± 3.96, $P = 0.2985$) and 35 dpi (control, 17.59 ± 2.09 *vs* diabetic, 23.25 ± 5.01, $P = 0.2940$) (Fig. 2I and J). Inflammatory foci/granulomas of diabetic mice appeared to be more diffuse and less compact than those of control mice (Fig. 2I and J). Moreover, compared to controls, bacilli in the liver of diabetic mice were not only localized within the inflammatory foci/granulomas, but were also found dispersed throughout the liver parenchyma.

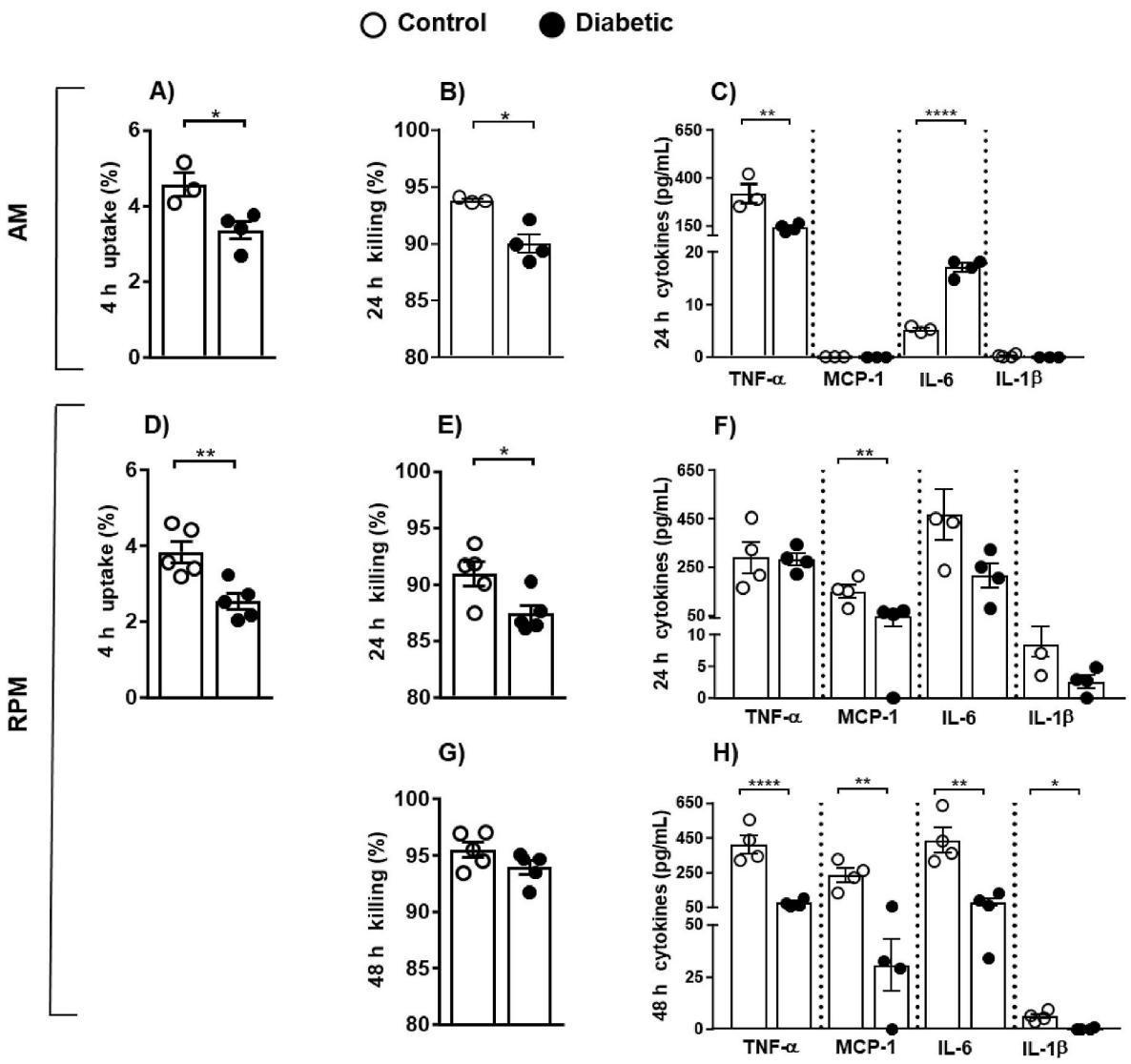

Fig. 1. Internalization and killing of *Mycobacterium bovis* BCG by alveolar and resident peritoneal macrophages are impaired in T2D. Macrophages from both diabetic and non-diabetic (control) mice were co-cultured with *Mycobacterium bovis* BCG at an MOI 1:10 for 4 and 24/48 h. *M. bovis* BCG uptake after 4 h (A) and killing of internalized bacteria after 24 h (B) were reduced significantly in alveolar macrophages (AM) from diabetic mice compared to controls. After 24 h of co-culture with the bacterium, there was a significant reduction of tumour necrosis factor-α (TNF-α) production by AM from diabetic mice compared to controls although an opposite trend was observed with interleukin-6 (IL-6) production (C). There was no or little production of monocyte chemoattractant protein-1 (MCP-1) and IL-1β by AM from both diabetic and controls at the same timepoint of co-culture (C). Similar to AM, there was a significant reduction of *M. bovis* BCG uptake (D) and 24 h killing (E) by resident peritoneal macrophages (RPM) from diabetic mice compared to controls. The 48 h killing of internalized mycobacteria were also lower in RPM from diabetic mice compared to controls albeit it was not statistically significant (G). After 24 h of co-culture, there was a significant reduction of MCP-1 production by the RPM from diabetic mice compared to controls although no differences were found in TNF-α secretion by RPM from both groups of mice (F). The production of IL-6 and IL-1β was lower in RPM from diabetic mice compared to controls at the same timepoint although these were not statistically significant (F). After 48 h of co-culture, the production of TNF-α, MCP-1, IL-6 and IL-1β were reduced significantly in RPM from diabetic mice compared to controls (H). The experiment was repeated twice with similar results. Result of a representative experiment was presented above. Data presented as mean ± SEM; n = 3–5 replicates at each timepoint. Level of significance: $*P \leq 0.05$, $**P \leq 0.01$ and $****P \leq 0.0001$.

3.5. Dysregulated cytokines in Mycobacterium bovis BCG-infected T2D mice

We next assessed the levels of inflammatory cytokines in lung and liver following *M. bovis* BCG infection. At 14 dpi, TNF-α levels were lower in diabetic lungs compared to controls (Fig. 3A). Whereas at 14 dpi MCP-1 production was significantly higher in diabetic lungs compared to controls (Fig. 3B). No significant changes in IL-1β and IL-6 production were observed between the two groups (Fig. 3C and D). IFN-γ was undetectable at 1 dpi but was significantly reduced in diabetic lungs compared to controls at both 14 and 35 dpi (Fig. 3E). In the liver similar trends were observed with TNF-α (Fig. 3F), and IFN-γ (Fig. 3J) being significantly lower in diabetic mice compared to controls at both 14 and 35 dpi and IL-6 (Fig. 3I) significantly lower in the same group at 35 dpi. IL-1β production was significantly higher in liver of diabetic mice although it was not significant for 14 and 35 dpi in the same group (Fig. 3H). IL-4 levels in diabetic livers were significantly higher compared to controls at 1 (control, 2.28 ± 1.53 *vs* diabetic, 7.85 ± 0.89, pg/mL, $P = 0.0198$) and 14 dpi (control, 2.29 ± 1.82 *vs* diabetic, 14.96 ± 4.45, pg/mL, $P = 0.0300$). The production of splenic MCP-1

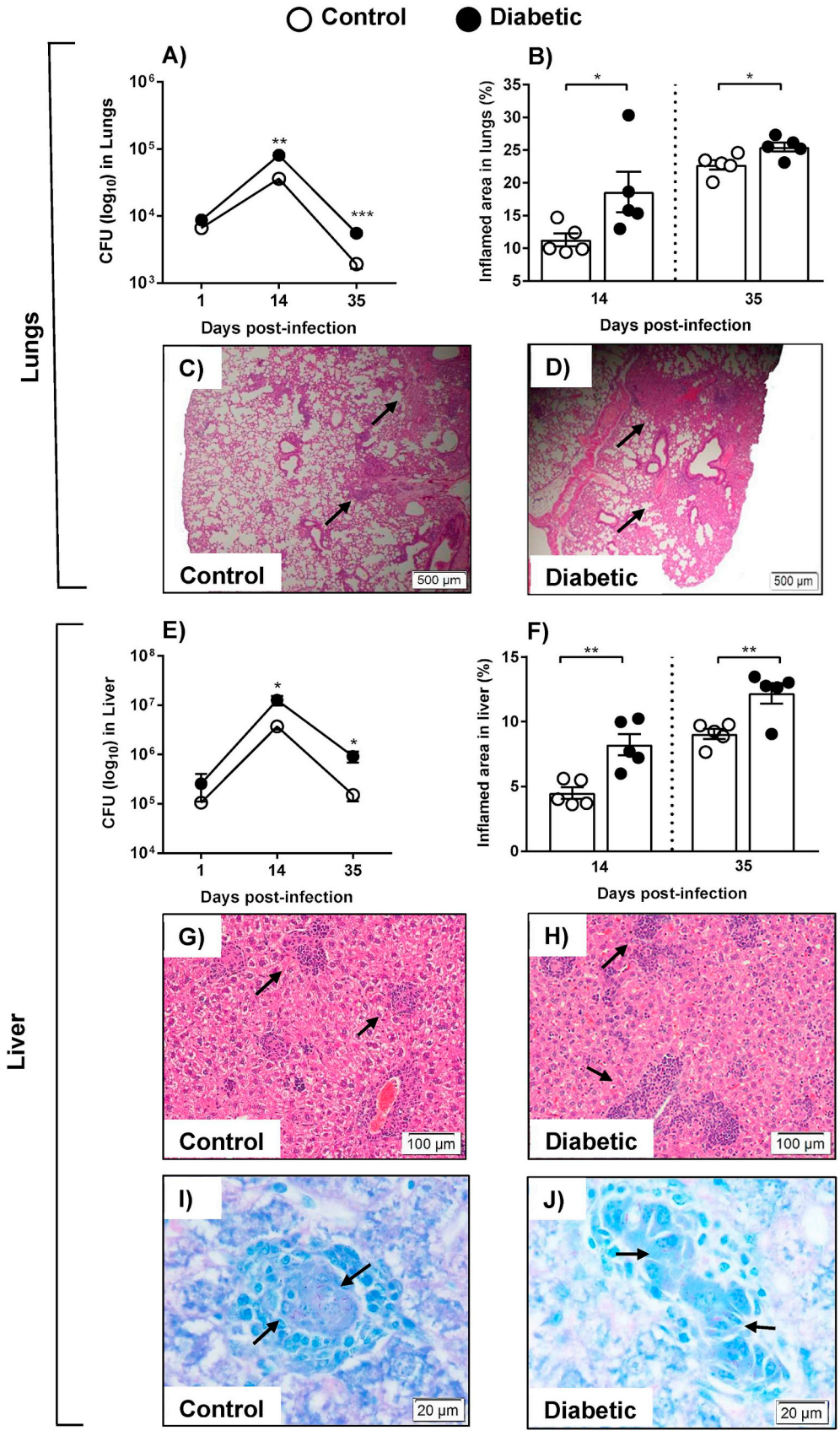

Fig. 2. Type 2 diabetes increases susceptibility to *Mycobacterium bovis* BCG infection. Diabetic and non-diabetic (control) mice were infected intravenously with *Mycobacterium bovis* BCG (1×10^6 CFU/mouse) and observed for a period of 35 days. Mice were sacrificed at 1, 14 and 35 days post-infection (dpi) and organ mycobacterial load and histopathological lesions were assessed. A significantly higher bacterial burden was observed in lung of diabetic mice compared to controls at 14 and 35 dpi (A). Histological examination and quantification of the inflammatory lesions indicated a higher inflamed area in lung of diabetic mice compared to controls (B, C and D). Similar to lung, significantly higher bacterial load (E) and inflammatory lesions (F, G and H) were observed in liver of diabetic mice compared to controls at 14 and 35 dpi. Ziehl-Neelsen staining of the same liver sections demonstrated higher numbers of *M. bovis* BCG in each inflammatory focus/granuloma of liver of diabetic mice compared to controls (I and J). Data presented as mean ± SEM; n = 4–5 mice/group at each timepoint. Figure C, D, G and J were the representative figures of 35 dpi timepoint. Magnification: C-D 40x (scale bar 500 µm), G-H 200x (scale bar 100 µm) and I-J 1000x (scale bar 20 µm). Level of significance: $*P \leq 0.05$, $**P \leq 0.01$ and $***P \leq 0.001$.

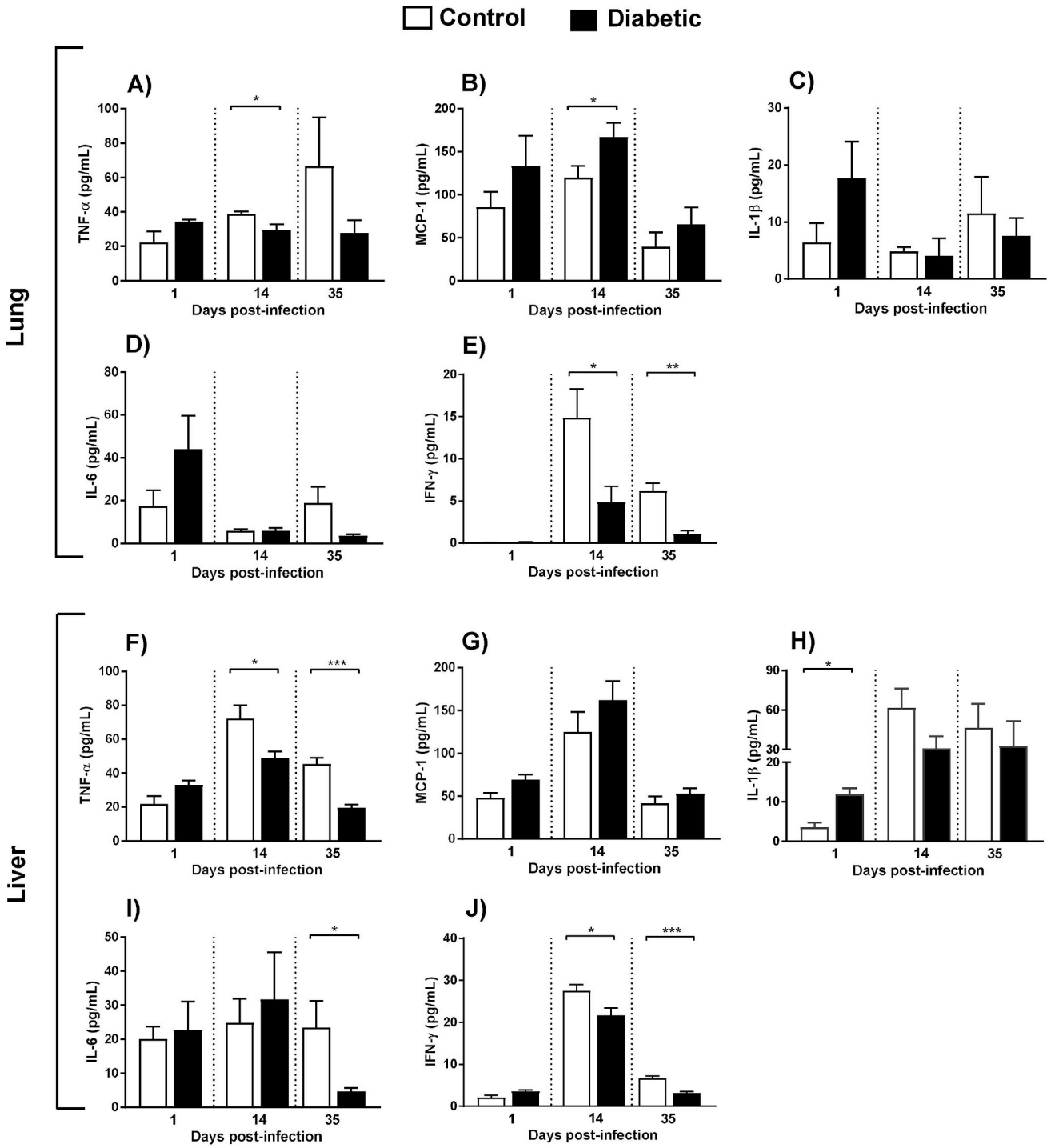

Fig. 3. Cytokine production is dysregulated in *Mycobacterium bovis* BCG infection in T2D. Mice were infected intravenously with *Mycobacterium bovis* BCG (1×10^6 CFU/mouse) and sacrificed at 1, 14 and 35 days post-infection (dpi) to determine cytokine production in the lung and liver. There was a significant reduction in the production of tumour necrosis factor-α (TNF-α) at 14 dpi in lungs of diabetic mice compared to non-diabetic controls (A). The production of monocyte chemoattractant protein-1 (MCP-1) was significantly higher in the lungs of diabetic mice compared to controls at 14 dpi (B). The production of interleukin (IL)-1β (C) and IL-6 (D) was not significantly different between the two groups. There were significantly lower levels of interferon-γ (IFN-γ) in the lungs of diabetic mice compared to controls at 14 and 35 dpi (E). Similar trends to the lungs in TNF-α (F), MCP-1 (G), IL-1β (H), IL-6 (I) and IFN-γ (J) production were observed in the liver of diabetic and controls. Data presented as mean ± SEM; n = 4–5 mice/group at each timepoint. Level of significance: $*P \leq 0.05$, $**P \leq 0.01$ and $***P \leq 0.001$.

at 35 dpi and IL-1β at 1 and 35 dpi were significantly higher in diabetics compared to controls (Supplementary Fig. 3). Whereas the production of IL-6 at 1 dpi, IFN-γ at 35 dpi and IL-2 at 14 and 35 dpi were significantly lower in the spleens of diabetic mice compared to controls (Supplementary Fig. 3).

4. Discussion

Identifying the immune mechanisms underlying TB-T2D co-morbidity is important for the development of effective therapeutic and preventive measures. Using a diet-induced animal model which reflects

the characteristics of T2D [3,21], this study investigated the anti-mycobacterial functions of mouse diabetic versus non-diabetic macrophages, and showed that diabetes influences animal survival and tissue bacterial burden, inflammation and cytokine levels following BCG infection.

Diabetic mice challenged with a high-dose of *M. bovis* BCG displayed a trend towards increased mortality. These results are consistent with other studies using Streptozotocin (STZ) induced diabetes followed by *M. tuberculosis* (*Mtb*) [13–15] and *M. fortuitum* infection [3]. In the current study, increased mortality was accompanied by a higher bacterial burden in the lung (Fig. 2A), liver (Fig. 2E) and spleen following a low-dose infection. A similar pattern of increased bacterial burden has been observed in STZ induced diabetic animals infected with *Mtb* [12,14–17,29,30]. The higher mycobacterial burden suggests that diabetic mice were unable to control infection efficiently. The increased bacterial burden in diabetic mouse tissue was further associated with increased inflammatory lesions in the lung (Fig. 2B, C and D) and liver (Fig. 2F, G and H). Previous studies have also reported an increased inflammation in lung [14–16] and liver [29,30] of STZ-induced diabetic animals infected with *Mtb*. The observed increase in bacterial burden in diabetic mice coupled with increased numbers and size of inflammatory lesions suggest a significant failure to control and confine the bacilli within the inflammatory lesions.

The increased bacterial burden and number and size of inflammatory lesions in diabetic mice, may be explained by impaired phagocytosis and/or dysregulated macrophage cytokine responses [3,17]. Macrophages are one of the first cell types to encounter mycobacteria within the lung [31,32]. Our study revealed significantly decreased uptake of *M. bovis* BCG by AM and RPM from diabetic mice (Fig. 1A and D). Defective uptake of *Mtb* by AM and *M. fortuitum* by both AM and RPM of diabetic mice has been described by others and us previously [3,18]. Reasons for the impaired diabetic phagocyte function may relate to reduced interactions between bacteria and phagocytes caused by altered complement protein (C3b) binding and/or receptor (CR1 and CR3) expression [33,34]. Furthermore, recent studies have demonstrated that diabetic macrophages have reduced expression of the scavenger receptor; macrophage receptors with collagenous structure (MARCO) [18] suggesting that both opsonin-dependent and -independent phagocytic process may be impaired in diabetics. The significantly reduced bacterial killing we observed for both diabetic AM (Fig. 1B) and RPM (Fig. 1E and G) may also be due to reduced secretion of antimycobacterial compounds, a delayed acidification of the phagosome and phagosome-lysosome fusion and altered cytokine secretion [31,32]. We observed reduced production of TNF-α by AM and RPM from diabetic mice (Fig. 1C and H). Our findings are consistent with previous studies in diabetic animals [3,29,30]. Decreased production of TNF-α by macrophages from diabetic animals was associated with lower uptake and killing of the bacilli. It is tempting to speculate that this could be due to the prominent role of TNF-α in the secretion of antimycobacterial compounds [35].

MCP-1 (CCL2) is a potent chemoattractant protein involved in recruiting various immune cells (including phagocytes) into infected tissue. Diabetic RPM produced less MCP-1 (Fig. 1F and H) suggesting an inability to recruit other immune cells. Vallerskog and colleagues [17] suggested a reduced level of MCP-1 as a cause of delayed recruitment of myeloid cells followed by delayed antigen presentation in *Mtb* infected diabetic mice. We observed higher levels of IL-6 produced by *M. bovis* BCG-infected diabetic AM (Fig. 1C) but lower levels in RPM (Fig. 1 F and H) compared to controls. Although there are conflicting reports on the role of IL-6 [36,37], the reduced IL-6 lead to higher bacterial survival. A higher level of *Mtb* growth in macrophages of IL-6 knockout mice has been observed previously [38]. Despite the lower production of IL-6 by AM, the increased production of TNF-α might compensate to limit bacterial growth. We also observed a reduced production of IL-1β by RPM from diabetic mice (Fig. 1F and H), which suggests that this cytokine is positively correlated with the secretion of TNF-α and IL-6 [39]. We detected a higher amount of IL-10 in RPM of control mice, although the survival of BCG inside the macrophages was low. The anti-inflammatory environment and increased killing of internalized bacteria by macrophages from non-diabetic mice may be compensated by elevated secretion of other pro-inflammatory cytokines (e.g. TNF-α, MCP-1, IL-6, IL-1β).

We observed significantly lower TNF-α production in the lung of BCG-infected diabetic mice at 14 dpi (Fig. 3A) which is consistent with our *in vitro* studies. In the liver, TNF-α was significantly reduced in diabetic mice at 14 and 35 dpi, and a similar trend was observed for IL-6 at 35 dpi (Fig. 3F and I). Similar findings have been reported in diabetic animal models following acute *Mtb* infections [15,29]. Lower production of these cytokines at the early stages of infection in diabetic mice failed to activate and recruit macrophages. Previous studies suggested that decreased production of cytokines in diabetic mice during mycobacterial infections leads to elevated bacterial burdens and increased inflammatory lesions [12,17]. Although MCP-1 production is crucial in mycobacterial defence, an increased production of this cytokine in diabetic mice at later timepoints failed to control bacillary loads, resulting in greater tissue inflammation [14,15,17]. We also observed low amounts of IFN-γ from the lung, liver (Fig. 3E and J) and spleen (Supplementary Fig. 3E) of diabetic mice compared to controls. The central role of Th1 cells in the defence against *Mtb* has been attributed to the ability of Th1 cell-derived IFN-γ to activate macrophages and stimulate phagocytosis, phagosome maturation, production of pro-inflammatory cytokines (e.g. TNF-γ, IL-1β, IL-6) and antigen presentation [31,32]. A decreased level of IFN-γ in response to BCG infection observed in this study (Fig. 3E and J) suggests impaired/delayed Th1 cell responses and leucocyte recruitment in diabetic mice. Previous research in hyperglycaemic mice have demonstrated that *Mtb*-specific IFN-γ producing T cell recruited later in the regional lymph nodes with a proportionate delay in recruitment of those cells to the lung leading to delayed T cell priming [17]. Reduced production of this cytokine may be further explained by the decreased production of IL-2 (Supplementary Fig. 3F) that could further reduce, or at least, delay Th1 cell differentiation and recruitment as seen in TB defence [31,32]. We also observed minor increases in IL-4 in the liver of diabetic mice early in infection suggesting the possibility that the immune response may be skewed towards a more Th2 cell type. IL-4 may induce macrophages to take on a M2 (alternatively activated) phenotype [31,32]. This may down-regulate Th1 responses by inhibiting Th1 cell differentiation via influencing the transcription of IFN-γ in Th1 effector cells [40]. Future studies are required to evaluate the role of this cytokine in diabetes-mycobacterial co-morbid infections.

Our work also suggests that delays or defects in the formation of inflammatory/granulomatous foci in the diabetic mice may be due to impaired macrophage activity. The observation of loosely associated cells in such foci and the diffusely spread bacilli in the liver parenchyma (Fig. 2J) suggests a possible impairment in leucocyte recruitment in response to higher numbers of bacilli. In contrast, inflammatory foci/granulomas of non-diabetic mice were more compact containing lower numbers of bacteria (Fig. 2I). In patients with TB who are immunodeficient, granulomas are larger in size, rich in activated macrophages with fewer surrounding lymphocytes in contrast to immunocompetent patients with TB who have small, compact granulomas with more IFN-γ producing $CD4^+$ T cells [41]. Future studies using relevant murine models should be aimed at characterizing the composition of the inflammatory foci/granulomas in the diabetic and non-diabetic mice.

In conclusion, impaired macrophage function is one of the key factors responsible for increased susceptibility to mycobacteria in diabetes, which ultimately leads to delayed Th1 cell mediated responses. In this investigation, we demonstrated that uptake, killing and cytokine production of macrophages from diabetic mice are impaired in early *M. bovis* BCG infection. These impairments lead to increased organ mycobacterial loads with defective or poor inflammatory or granulomatous

foci formation in diabetes due to impaired or defective Th1 cell responses. We consider the model we have developed and characterized in terms of early responses in T2D to mycobacterial infection is robust, and therefore appropriate to further investigate the impairment in development of protection in T2D-mycobacterial co-morbidity.

Conflicts of interest

There are no conflicts of interest relevant to this manuscript.

Ethical approval

All animal experiments were conducted following the National Health and Medical Research Council (NHMRC) guidelines and approved by the institutional Animal Ethics Committee (A2016).

Acknowledgements

The authors wish to thank Associate Professor Leigh Owens, College of Public Health, Medical and Veterinary Sciences and Dr. A. B. M. Rabiul Alam Beg, College of Business, Law and Governance of James Cook University for their advice and guidance in statistical analysis. Md Abdul Alim is a faculty member of Chittagong Veterinary and Animal Sciences University, Bangladesh and a recipient of an Endeavour Postgraduate Scholarship (PhD) from the Australian Government, Department of Education and Training.

Appendix A. Supplementary data

Supplementary data to this article can be found online at https://doi.org/10.1016/j.tube.2019.02.005.

Funding

This research was supported by James Cook University internal grants awarded to Natkunam Ketheesan, Brenda L Govan and Catherine M Rush.

References

[1] Smyth S, Heron A. Diabetes and obesity: the twin epidemics. Nat Med 2006;12(1):75–80.
[2] Jeon CY, Murray MB. Diabetes mellitus increases the risk of active tuberculosis: a systematic review of 13 observational studies. PLoS Med 2008;5(7):e152.
[3] Alim MA, et al. Anti-mycobacterial function of macrophages is impaired in a diet induced model of type 2 diabetes. Tuberculosis (Edinb) 2017;102:47–54.
[4] Bridson T, et al. Overrepresentation of diabetes in soft tissue nontuberculous mycobacterial infections. Am J Trop Med Hyg 2016;95(3):528–30.
[5] Hensel RL, et al. Increased risk of latent tuberculous infection among persons with pre-diabetes and diabetes mellitus. Int J Tuberc Lung Dis Offic J Int Union Tuberc Lung Dis 2016;20(1):71–8.
[6] Trunz BB, Fine P, Dye C. Effect of BCG vaccination on childhood tuberculous meningitis and miliary tuberculosis worldwide: a meta-analysis and assessment of cost-effectiveness. Lancet 2006;367(9517):1173–80.
[7] Colditz GA, et al. Efficacy of BCG vaccine in the prevention of tuberculosis. Meta-analysis of the published literature. Jama 1994;271(9):698–702.
[8] Sharpe S, et al. Alternative BCG delivery strategies improve protection against Mycobacterium tuberculosis in non-human primates: protection associated with mycobacterial antigen-specific CD4 effector memory T-cell populations. Tuberculosis (Edinb Scotl) 2016;101:174–90.
[9] Anacker RL, et al. Superiority of intravenously administered BCG and BCG cell walls in protecting rhesus monkeys (Macaca mulatta) against airborne tuberculosis. Z für Immunitatsforsch Exp Klin Immunol 1972;143(4):363–76.
[10] Barclay WR, et al. Aerosol-induced tuberculosis in subhuman primates and the course of the disease after intravenous BCG vaccination. Infect Immun 1970;2(5):574–82.
[11] Cefalu WT. Animal models of type 2 diabetes: clinical presentation and pathophysiological relevance to the human condition. ILAR J 2006;47(3):186–98.
[12] Yamashiro S, et al. Lower expression of Th1-related cytokines and inducible nitric oxide synthase in mice with streptozotocin-induced diabetes mellitus infected with Mycobacterium tuberculosis. Clin Exp Immunol 2005;139(1):57–64.
[13] Saiki O, et al. Depressed immunological defence mechanisms in mice with experimentally induced diabetes. Infect Immun 1980;28(1):127–31.
[14] Podell BK, et al. Increased severity of tuberculosis in Guinea pigs with type 2 diabetes: a model of diabetes-tuberculosis comorbidity. Am J Pathol 2014;184(4):1104–18.
[15] Cheekatla SS, et al. NK-CD11c+ Cell Crosstalk in Diabetes Enhances IL-6-Mediated Inflammation during Mycobacterium tuberculosis Infection. PLoS Pathog 2016;12(10):e1005972.
[16] Martens GW, et al. Tuberculosis susceptibility of diabetic mice. Am J Respir Cell Mol Biol 2007;37(5):518–24.
[17] Vallerskog T, Martens GW, Kornfeld H. Diabetic mice display a delayed adaptive immune response to Mycobacterium tuberculosis. J Immunol 2010;184(11):6275–82.
[18] Martinez N, et al. Impaired recognition of Mycobacterium tuberculosis by alveolar macrophages from diabetic mice. J Infect Dis 2016;214(11):1629–37.
[19] Surwit RS, et al. Diet-induced type II diabetes in C57BL/6J mice. Diabetes 1988;37(9):1163–7.
[20] Hodgson K, et al. Dietary composition of carbohydrates contributes to the development of experimental type 2 diabetes. Endocrine 2013;43(2):447–51.
[21] Morris JL, et al. Development of a diet-induced murine model of diabetes featuring cardinal metabolic and pathophysiological abnormalities of type 2 diabetes. Biol Open 2016;5(8):1149–62.
[22] Ayala JE, et al. Standard operating procedures for describing and performing metabolic tests of glucose homeostasis in mice. Dis Model Mech 2010;3(9–10):525–34.
[23] Larsen MH, Biermann K, Jacobs Jr. WR. Laboratory maintenance of Mycobacterium tuberculosis. Curr Protoc Microbiol 2007. https://doi.org/10.1002/9780471729259.mc10a01s6 [Chapter 10]: p. Unit 10A.1.
[24] Orme IM, Roberts AD. Animal models of mycobacteria infection. Curr Protoc Immunol 2001. https://doi.org/10.1002/0471142735.im1905s30 [Chapter 19]: p. Unit 19.5.
[25] Ordway DJ, Orme IM. Animal models of mycobacteria infection. Curr Protoc Immunol 2011. https://doi.org/10.1002/0471142735.im1905s94 [Chapter 19]: p. Unit19.5.
[26] Kupz A, et al. ESAT-6-dependent cytosolic pattern recognition drives noncognate tuberculosis control in vivo. J Clin Invest 2016;126(6):2109–22.
[27] Flynn JL, et al. Effects of aminoguanidine on latent murine tuberculosis. J Immunol 1998;160(4):1796–803.
[28] Chambers MA, Gavier-Widen D, Hewinson RG. Histopathogenesis of experimental Mycobacterium bovis infection in mice. Res Vet Sci 2006;80(1):62–70.
[29] Sugawara I, Yamada H, Mizuno S. Pulmonary tuberculosis in spontaneously diabetic goto kakizaki rats. Tohoku J Exp Med 2004;204(2):135–45.
[30] Sugawara I, Mizuno S. Higher susceptibility of type 1 diabetic rats to Mycobacterium tuberculosis infection. Tohoku J Exp Med 2008;216(4):363–70.
[31] Cooper AM, Mayer-Barber KD, Sher A. Role of innate cytokines in mycobacterial infection. Mucosal Immunol 2011;4(3):252–60.
[32] Cooper AM. Cell-mediated immune responses in tuberculosis. Annu Rev Immunol 2009;27:393–422.
[33] Schlesinger LS, et al. Phagocytosis of Mycobacterium tuberculosis is mediated by human monocyte complement receptors and complement component C3. J Immunol 1990;144(7):2771–80.
[34] Gomez DI, et al. Reduced Mycobacterium tuberculosis association with monocytes from diabetes patients that have poor glucose control. Tuberculosis (Edinb) 2013;93(2):192–7.
[35] Yu K, et al. Toxicity of nitrogen oxides and related oxidants on mycobacteria: M. tuberculosis is resistant to peroxynitrite anion. Tuber Lung Dis 1999;79(4):191–8.
[36] Sodenkamp J, et al. Therapeutic targeting of interleukin-6 trans-signaling does not affect the outcome of experimental tuberculosis. Immunobiology 2012;217(10):996–1004.
[37] Ladel CH, et al. Lethal tuberculosis in interleukin-6-deficient mutant mice. Infect Immun 1997;65(11):4843–9.
[38] Martinez AN, Mehra S, Kaushal D. Role of interleukin 6 in innate immunity to Mycobacterium tuberculosis infection. J Infect Dis 2013;207(8):1253–61.
[39] Dinarello CA. Interleukin-1 beta. Crit Care Med 2005;33(12 Suppl):S460–2.
[40] Wurtz O, Bajenoff M, Guerder S. IL-4-mediated inhibition of IFN-gamma production by CD4+ T cells proceeds by several developmentally regulated mechanisms. Int Immunol 2004;16(3):501–8.
[41] Ulrichs T, et al. Differential organization of the local immune response in patients with active cavitary tuberculosis or with nonprogressive tuberculoma. J Infect Dis 2005;192(1):89–97.